IAEA
INTERNATIONAL ATOMIC ENERGY AGENCY

20th IAEA Fusion Energy Conference

Vilamoura, Portugal, 1-6 November 2004

IAEA-CN-116/EX/P6-20

Density Profile Evolution during Dynamic Processes in ASDEX Upgrade

I. Nunes 1), J. Santos 1), F. Salzedas 1), M. Manso 1), F. Serra 1), G. D. Conway 2), L. D. Horton 2), J. Neuhauser 2), W. Suttrop 2), and the CFN 1) and the ASDEX Upgrade 2) Teams

1) Centro de Fusão Nuclear, Associação EURATOM/IST, Lisboa, Portugal
2) Max-Planck Institut für Plasmaphysik, EURATOM-Association IPP, Garching, D-85748, Germany

Density Profile Evolution during Dynamic Processes in ASDEX Upgrade

I. Nunes 1), J. Santos 1), F. Salzedas 1), M. Manso 1), F. Serra 1), G. D. Conway 2), L. D. Horton 2), J. Neuhauser 2), W. Suttrop 2), and the CFN 1) and ASDEX Upgrade 2) Teams

1) Centro de Fusão Nuclear, Associação EURATOM-IST, Lisboa, Portugal
2) Max-Planck Institut für Plasmaphysik, EURATOM-Association IPP, Garching D-85748, Germany

email contact of main author: inunes@cfn.ist.utl.pt

Abstract. The current understanding of edge localized modes (ELMs) and the trigger of major disruptions is largely based on phenomenology. The need to better understand the processes underlying these phenomena requires high temporal and spatial resolution diagnostics. Fast diagnostics for the temperature measurements exist, such as the ECE radiometer but, for the plasma density, the existing diagnostics such as Lithium Beam and Thomson Scattering do not have the required high temporal resolution for a period long enough to characterize the entire ELM event. The microwave reflectometry system on ASDEX Upgrade has the capability to measure electron density profiles simultaneously at the low-field and high-field sides, in broadband swept ultrafast (35μs) operation with a spatial resolution of 5mm. In this paper we report on recent results on the effects of type I ELMs on density profiles and on the density pedestal width and ELM affected depth. During the ELM event, three phases are identified: precursor, collapse and recovery. The density pedestal width is found to be approximately constant for all the ELMy H-mode discharges analyzed here, except for high input power discharges, where an increase of the density pedestal width is observed. Major disruptions limit the range of parameters used in the operation of a tokamak, especially density limit disruptions, that limit the maximum usable density. Very abrupt increases of density are observed before the onset of the electron temperature profile erosion, supporting the hypothesis that this erosion is due to convection of the magnetic field. In ITER, during the long steady state flat-top phase of the discharges magnetic measurements may accumulate significant drifts. Plasma position and shape control using reflectometry is being assessed in ASDEX Upgrade for ITER like scenarios with successful results, where it is shown that position measurements from reflectometry compared to magnetic data satisfy the ITER requirements. Combined simulated and experimental data determine the position of the separatrix within 1 cm.

1. Introduction

The ultrafast reflectometer system installed at ASDEX Upgrade measures density profiles (n_e) with high temporal (35μs) and spatial resolution ($\sim$5 mm). With O-mode the probed densities can reach $\sim 12 \times 10^{19}\mathrm{m}^{-3}$ on the low-field side and $\sim 6 \times 10^{19}\mathrm{m}^{-3}$ on the high-field side[1]. This paper focus on the dynamics of the edge localized modes (ELMs), namely the precursor, collapse and recovery phase, and on the density pedestal width (Δ_{ne}) and edge density gradient ($\bigtriangledown n_e$), for a series of discharges where several plasma parameters were varied at fixed magnetic field of 2T. Due to the fast sweep repetition period, several entire ELM cycles with a typical frequency $\sim$ 100Hz can be characterized. Also discussed here is the comparison of the experimental Δ_{ne} and $\bigtriangledown n_e$ values with those predicted by the neutral penetration model [2,3]. The scanned param-

eters are the plasma current (I_p = 0.6, 0.8, 1.2 MA), triangularity (δ = 0.27 (DOC-L); 0.32 (EOC); 0.44 (HT3)), input power (P_{IN} = 2.4; 5.2; 8.3 MW) and plasma density by fuelling, which leads to an overall variation of the pedestal density of $n_{e,ped}$ = 3-7 $\times 10^{19}$ m^{-3}. The ultrafast reflectometer also allows the study of the physical mechanisms of the fast destruction of energy confinement that trigger major density limit disruptions. For this study, also a set of dedicated experiments was performed [4]. The density profiles from reflectometry, measured throughout the disruption, showed very abrupt increases in density preceding the onset of the erosion of the electron temperature (T_e) profiles. The T_e erosion starts from the O point of the $m/n = 2/1$ magnetic island and advances towards the plasma core (as observed also at RTP and JET). These observations support the hypothesis that the erosion of electron temperature is due to convection and not by stochastization of the magnetic field due to low m, n number MHD modes interaction.

The information about the density profiles also provides a powerful tool for plasma position and shape control, as proposed for ITER to complement the magnetic measurements. A set of four or more reflectometers at different poloidal locations are planned to measure the plasma-wall gaps that will be supplied to the position and shape control system. The position of the separatrix is found from the measured density profiles by using a scaling factor derived from the line average density and the density at the separatrix. A comprehensive assessment of the quality of such measurements has been made in the ITER reference scenario, the ELMy H-mode. The validation of the errors in the position of the separatrix is assessed by using a 1D numerical simulation and experimental data from the ASDEX Upgrade tokamak for a ITER like scenario. The estimated position of the separatrix is found within 1 cm of accuracy when compared to the separatrix position derived from magnetic data.

This paper is organized as follows. The experimental results are given in sections 2 to 6, where section 2, 3 and 4 describe the experimental results on the effects of type I ELMs on the density profiles, including the results on the ELM affected depth and the density pedestal width and gradient. In section 5 the behaviour of the density profiles during major density limit disruptions is discussed and in section 6 the experimental results on the plasma position and shape control are described. Finally a summary and conclusions are given in section 7.

2. ELM dynamics

From the analysis of the density profile evolution during an ELM event, three characteristic phases of the ELM can be defined: precursor, collapse and recovery [5] for both the low-field (LFS) and the high-field (HFS) sides. A similar definition for the ELM dynamics at the LFS has also been proposed by JT-60U [6]. During the precursor phase, low frequency oscillations starting approximately 3 ms prior to the ELM collapse are observed in the density profiles. Density fluctuation measurements show a continuous rise of the broadband fluctuations prior to the ELM collapse as shown in figure 1. At the collapse phase, coincident with the period of enhanced MHD activity, the crash of the density profile is observed. After the density crash the density pedestal has moved inwards while the density profile at the scrape-off layer broadens defining a radial pivot point as shown in figure 2(a).

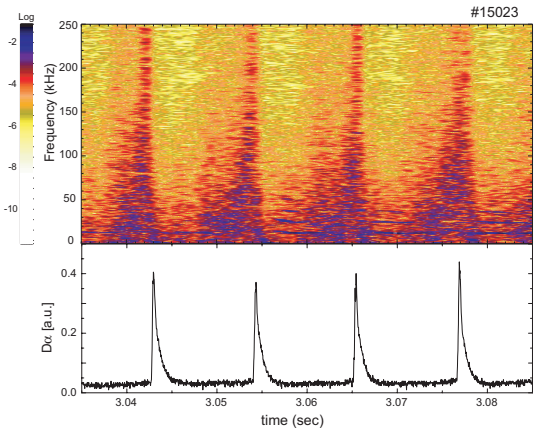

Figure 1: *Spectrogram of a fixed frequency channel measuring at* $n_e = 2.98 \times 10^{19} m^{-3}$.

The density in the two regions around the pivot point is observed to behave differently during the recovery phase. Inside the radial pivot point, the recovery time seems to be correlated with the ELM frequency while, outside the radial pivot point, no correlation is found with the recovery time that is around 2-4 ms as shown in figure 2(b) for all ELM frequencies. The different behaviour of the density in the two regions indicates that the processes by which the plasma recovers its initial pre-ELM shape are different. The observed correlation between the pedestal recovery time and the ELM period suggests a dependence on how much the density collapses due to the ELM and hence the number of particles lost during the ELM event.

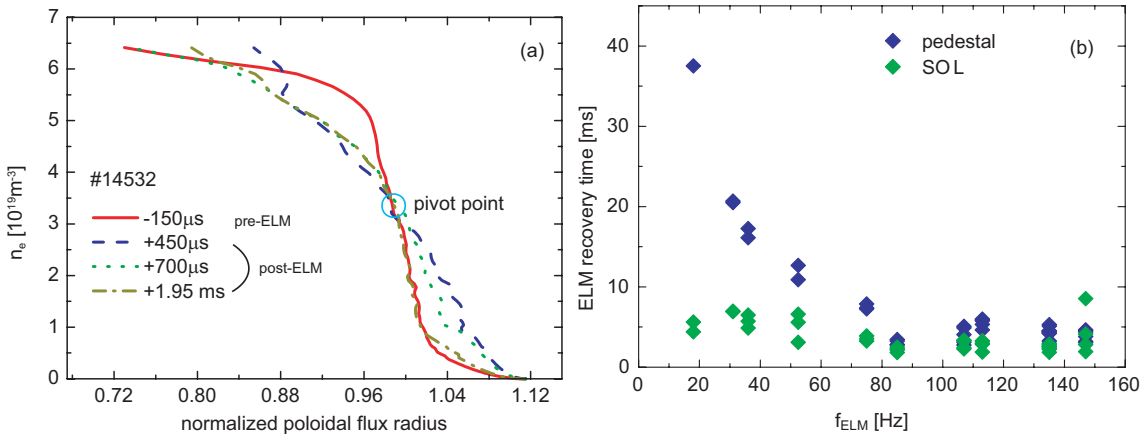

Figure 2: *(a) Time evolution of the density profiles before and after an ELM event; (b) Pedestal and SOL recovery time as a function of the ELM period.*

3. ELM affected depth

The ELM affected depth is determined as the distance between the pivot point and the innermost point, where the effect of the ELM on the density is not observed anymore (points A and B in figure 3 (a) respectively). It is found that the ELM affected depth on the density profiles remains fairly constant with the pedestal density (normalized to the Greenwald limit) up to densities $\leq 0.55 n_{GW}$ while above this value the ELM affected depth decreases slightly. A similar result is found for the ELM particle losses, $(\Delta N_{ELM}/n_{e,ped}V_p)$. No clear trend is observed for pedestal densities below $0.55 n_{GW}$, while for higher densities the ELM particle losses also decrease slightly, similar to the results reported by DIII-D [7]. Figure 3 (b) shows the ELM affected depth as a function of the ELM particle losses where both are seen to change in a correlated way, showing a strong dependence on how much the plasma is affected by the ELM and a weak dependence on the plasma parameters before the ELM such as triangularity.

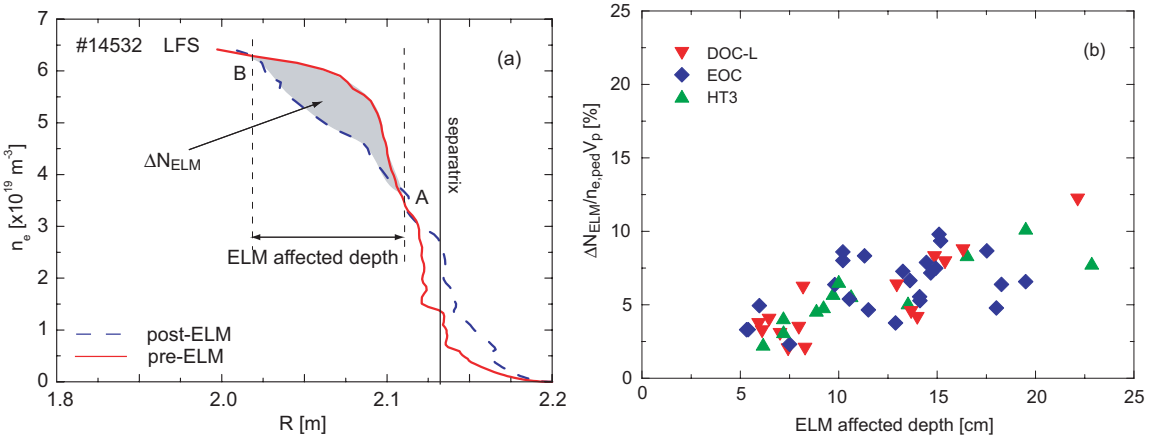

Figure 3: *(a) The ELM affected depth (density) due to an ELM is defined as the region between the pivot point (A) and the innermost point where the effect of the ELM in the density is not seen (B). The region where the particles losses, ΔN_{ELM} is also defined. (b) ELM affected depth as a function of the ELM particle losses (normalized to the plasma particle content).*

4. Density pedestal width and gradient

The density pedestal width and gradient is determined for the same set of dis-

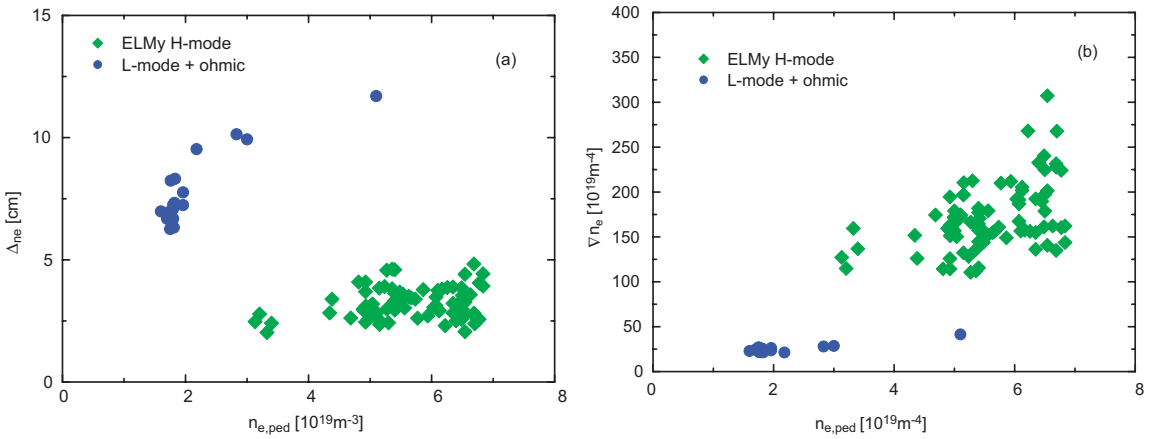

Figure 4: *(a) Density pedestal width and (b) edge gradient as a function of $n_{e,ped}$ for ELMy H-mode, L-mode and ohmic phases.*

charges defined above. Shown in figure 4 is (a) the density pedestal width and (b) the edge density gradient as a function of the varied plasma parameters $(I_p, n_e, P_{IN}, \delta)$. The density pedestal width does not change significantly with the main plasma parameters (used in this study), with values around 2-3.5 cm. On the other hand, the edge density gradient changes significantly with density and plasma current ($\propto I_p^2$). The density pedestal width and gradient is also determined for ohmic and L-mode discharges and compared with the H-mode discharges values. Although L-mode and ohmic regimes do not have an ETB, a pedestal is observed in the density profiles (figure 5). A comparison between L- and H-mode discharges with similar pedestal density shows that Δ_{ne} for L-mode is about a factor 3 higher than that of the H-mode and $\bigtriangledown n_e$ is about 3 times

smaller. Also, for ohmic and L-mode phases, the density pedestal width increases with density, contrary to H-mode phases where it stays approximately constant.

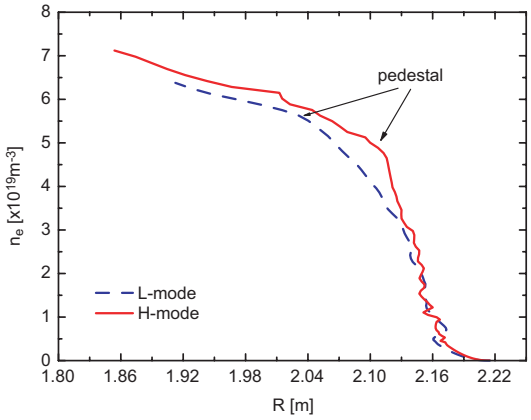

Figure 5: *H- and L-mode density profiles showing both a density pedestal.*

The only model put forward to explain the formation of the ETB is the neutral penetration model, where Δ_{ne} is found to be proportional to $1/n_{e,ped}$ and $\bigtriangledown n_e$ is proportional to $n^2_{e,ped}$ independently of the confinement regime, L- or H-mode [2]. Although in DIII-D the estimated values given by the neutral penetration model agree with the experimental values of Δ_{ne} and $\bigtriangledown n_e$ [7], the same is not observed in ASDEX Upgrade data for this set of discharges. From figure 4(a) is clearly seen that for the same pedestal density, the experimental values of Δ_{ne} for an L-mode discharge and an H-mode discharge differ significantly, suggesting that is not the neutral penetration by itself that defines the width of the ETB [8].

5. Density limit disruptions

These experiments were performed in lower single null diverted ohmic plasmas with $I_p = 1$ MA and $B_T = 2.4$ T to obtain a $q_{95} = 4$. An ohmic density limit with $n_e = 6 \times 10^{19}$ m^{-3} was achieved by puffing neon gas on a deuterium plasma, in order to lower the density limit, relatively to a Deuterium plasma. The electron temperature profiles were evaluated from the ECE radiometer, measuring at the LFS, with a temporal resolution of 32 μs. The ohmic density limit disruptions studied here showed typical features of other ASDEX Upgrade density limit disruptions [9]. In the precursor, a MARFE is observed at 2.3632s forming in the divertor region and moving up towards the midplane via the HFS. At $\sim$ 3 s it eventually decays into a poloidally symmetric radiation shell. The increased edge radiation leads to an unstable current profile that destabilizes an $m/n = 2/1$ tearing mode at $R_{LFS} \approx 2$ m, as shown in figure 6(d). At 3.06 s the 2/1 mode locks to the wall with the O point in front of the ECE radiometer antenna. The cold plasma region expanding from

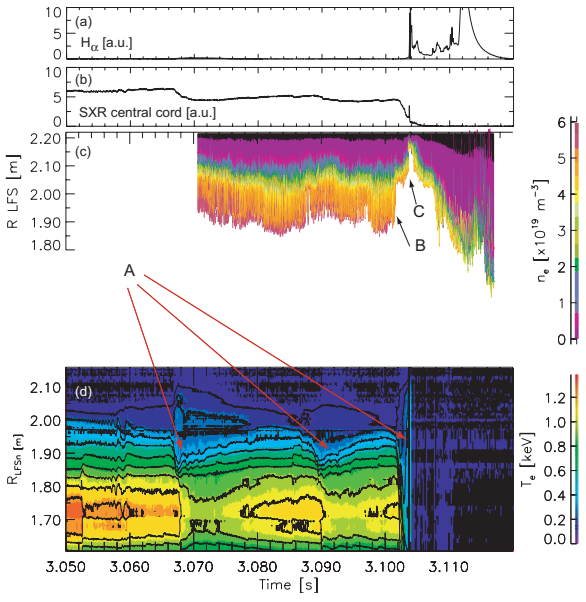

Figure 6: *Synchronized plots of plasma parameters. (a) H_α emission, (b) SXR emission (c) low-field side density profiles and (d) electron temperature profiles.*

the LFS mode's O point towards the plasma core is very similar to the 2/1 O point T_e erosion previously observed in RTP [10]. Seven ms later a minor disruption occurs. After this minor disruption there is one other smaller minor disruption at 3.09 s before the major disruption at 3.103 s (arrows A).

The reflectometer starts to measure at 3.07 s missing the first minor disruption. The density profile evolution shows that the start of the 2/1 T_e erosion, starting from the core facing side of the rational surface, occurs together with an abrupt and consistent increase in the density profile around $q = 2$ surface at the LFS, as shown by arrow B in figure 6(c). The final collapse of the temperature occurs when the density at the LFS peaks even further (arrow C in figure 6(c)). At the same instant, a peak in the H_α emission at the divertor (figure 6(a)) and in the SXR emission (figure 6(b)) is observed.

The reflectometer measures the density along an horizontal chord or more precisely, it measures the position of the cut-off layer for the probing frequency. This prevents any detection of a density decrease behind the cut-off layer. However, comparing these observations with those at RTP [9] (where the energy quench shows very similar features), it is presumed that these abrupt changes in the density profile are local perturbations moving radially outwards.

6. Plasma position and shape control

Reflectometry has been proposed to supply plasma-wall gap measurements to the ITER position and shape control system, during the long steady state flat-top phase of the discharges. First successful results [11] were obtained in typical plasma scenarios using the ASDEX Upgrade O-mode reflectometer. Figure 7(b) shows the evolution of

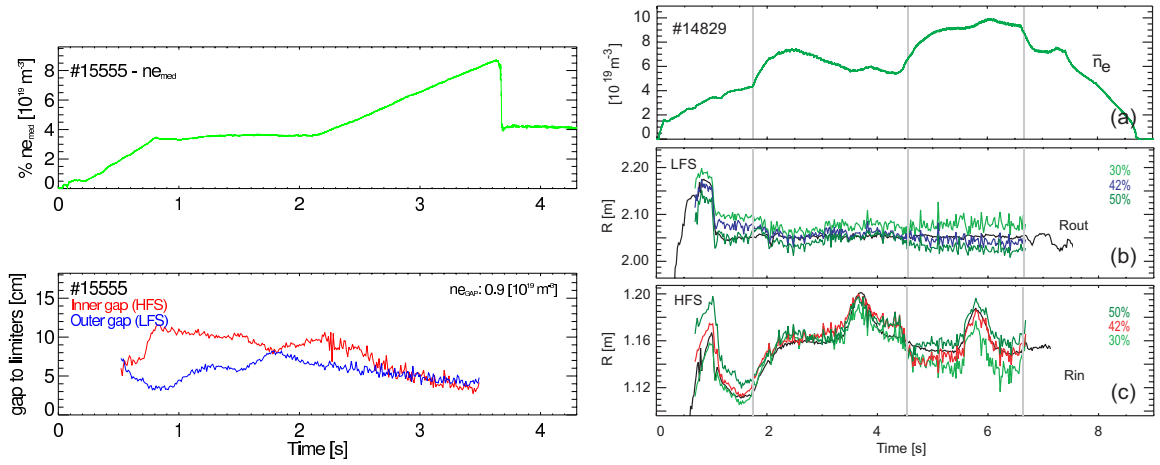

Figure 7: *(a) Evolution of the plasma-wall gap of a density layer* $n_e = 0.9 \times 10^{19} m^{-3}$ *during a density limit discharge with a radial scan (1.5-2.1 s). (b) Evolution of the estimate of the separatrix position for* $n_{e,sep}$ *= 0.30* n_e*, 0.42* n_e*, 0.50* n_e *during a standard ELMy H-mode discharge with* I_p*=1 MA. The position of the magnetic separatrix (*R_{in} *and* R_{out} *curves) is shown in black.*

a fixed density layer gap to the limiters on a standard density limit discharge (a radial scan of the plasma column was performed for t=1.5-2.1 s). Provided that density is constant within the magnetic flux surfaces, a scaling factor between the line average density and the density at the separatrix, $n_{e,sep}$, can be used to estimate $n_{e,sep}$ from

online line average density measurements. The separatrix position can then be inferred from the measured density profiles. The time evolution of such an estimation for several scaling factors is shown in figure 7(b) for an ASDEX Upgrade standard H-mode discharge and compared to the magnetics data. A preliminary assessment of the quality of such measurements has been made in the ITER reference scenario, the ELMy H-mode. For the reflectometer, this scenario is very demanding since the ELMs cause large and abrupt changes of the plasma edge density profile as well as strong density fluctuations. Confidence built with a successful validation of these tools in ASDEX Upgrade, where ITER relevant scenarios are regularly tested, is crucial for the extrapolation of the results to ITER where a multiple channel setup is planned. With the LFS and HFS reflectometers of ASDEX Upgrade, we were able to infer the position of two points of the plasma separatrix using adequate ratios between the linear average density and the density at separatrix. It was shown that the estimated separatrix positions satisfy the ITER requirements for position measurements (1 cm accuracy) when compared to similar magnetic data [12] even in phases when the pedestal density is out of the measuring range. Measurements during the onset and MHD phase of the ELMs, however, have to be discarded. During these phases the external transport barrier is lost and the estimation of the separatrix by means of such a scaling factor becomes unusable. The high temporal resolution of the reflectometer in ASDEX Upgrade, largely compensates for the measurement discarding, especially when compared to the ITER required time resolution of 10 ms.

7. Summary

With high spatial and temporal resolution reflectometry, a detailed characterization of the plasma density behaviour during fast dynamic processes such as ELMs and density limit disruptions is possible, as shown here. From the analysis of the density profile dynamics three different phases of the ELM dynamics have been identified and characterized; precursor, collapse and recovery. After the crash of the profile, a pivot point close (inside) the separatrix defines two regions. The ELM affected depth is $\sim$20-40% of the minor plasma radius for the range of densities 3-7 $\times 10^{19}$ m^{-3}. No clear dependence with the plasma parameters varied in these experiments is observed. The density pedestal width is found to be independent of the plasma parameters varied here $(n_e, I_p, \delta, P_{IN})$. It is found to be approximately constant in a range of 2-3.5 cm. The density gradient is seen to vary strongly with triangularity and plasma current, in line with the increase of the ballooning limit allowing steeper edge gradients and therefore higher tokamak performance. A comparison between a high density L-mode discharge and an ELMy H-mode discharge where the pedestal density is similar shows that the density pedestal width for the high density L-mode discharge is about three times larger than the one obtained for the H-mode discharge. These results show that the neutral penetration model does not explain the pedestal width measurements in ASDEX Upgrade, at least for these set of discharges.

The measurements of the density profiles during a density limit disruption showed very abrupt increases in density, preceding the onset of the erosion of the electron temperature T_e profile. The T_e erosion followed a pattern very similar to the one observed in RTP [4] e JET [4], i.e. it starts from the O point of the m/n=2/1 mode and advances towards the plasma core. As postulated in [4], these observations support the idea that the erosion of T_e is due to convection and not by stochastization of the magnetic field due to low m, n number MHD modes interaction.

The plasma position measurements obtained in ASDEX Upgrade with microwave

reflectometry both in density limit and ELMy H-mode discharges are in good agreement with similar data inferred from the standard magnetic diagnostics. These results give a good indication about the reliability of the reflectometry measurements. As the analysis performed was completely automatic, the study shows that it will be possible to use reflectometry to obtain routinely position measurements. The fact that the experiments were performed in ITER relevant plasma scenarios with transient events like ELMs and large variations of the average density gives a considerable operational experience for this new application of reflectometry.

References

[1] SILVA A. et al., Rev. Sci. Instrum. **67**, (1996) 4138
[2] ENGELHARDT, W. et al., J. Nucl. Mat., **76-77**, (1978) 518
[3] MAHDAVI, M. et al., Nucl. Fusion, **42**, (2002) 52
[4] SALZEDAS, F. et al, Proceedings of the 29^{th} EPS Conf. on Control. Fusion and Plasma Phys. (Montreux), (2002) ECA Vol. **26B** P-1.039
[5] NUNES, I. et al., Nucl. Fusion **44** (2004) 883
[6] OYAMA, N. et al., Plasma Phys. and Control. Fusion, **43**, (2001) 717
[7] GROEBNER, R. J. et al., Plasma Phys. and Control. Fusion, **44**, (2002), A265
[8] HORTON, L. D. et al., IAEA-CN-116/EX/P3-4 this conference
[9] SALZEDAS, F. et al., Phys. Plasmas **9** (2002) 3402
[10] SALZEDAS, F. et al, Proceedings of the 30^{th} EPS Conf. on Control. Fusion and Plasma Phys. (St. Petersburg), (2003) ECA Vol. **27A** P-2.95
[11] SANTOS, J. et al. Rev. Sci. Instrum. **74**, (2003) 1489
[12] SANTOS J. et al. Accepted for publishing in Rev. Sci. Instrum. (2004)